Desalination and Water Treatment
www.deswater.com

27 (2011) 159–166
March

1944-3994/1944-3986 © 2011 Desalination Publications. All rights reserved
doi: 10/5004/dwt.2011.2181

Electrochemical characterization of an ultrafiltration regenerated cellulose/polypropylene supported membrane

V. Romero, L. Peláez, M.I. Vázquez, J. Benavente*

Grupo de Caracterización Electrocinética y de Transporte en Membranas e Interfases, Departamento de Física Aplicada I, Facultad de Ciencias, Universidad de Málaga, E-29071 Málaga, Spain
Email: j_benavente@uma.es

Received 29 July 2010; Accepted 20 October 2010

ABSTRACT

Electrochemical characteristic parameters such as diffusional permeability, ion transport number, fixed charge concentration and electrical resistance for a regenerated cellulose/polypropylene-supported membrane (RC/PP sample) in contact with NaCl solutions at different concentrations were determined. The effect of the polypropylene support on mass and charge transport was estimated by comparing results obtained for both opposite fluxes and differences seem to be related to the stagnant solution layer embedded in the polypropylene support, which could mask membrane properties. Moreover, effective membrane thickness (RC-layer thickness) must be estimated to determine intensive membrane parameters (salt and ions diffusion coefficients or conductivity). Good agreement for ion diffusion coefficient values was obtained by comparing results obtained from different types of measurements (combination of membrane potential-salt diffusion and impedance spectroscopy, respectively).

Keywords: Electrochemical characterization; Salt diffusion; Membrane potential; Streaming potential; Impedance spectroscopy

1. Introduction

Membrane hydrodynamic and diffusional permeabilities, (L_p and P_s, respectively) are the two parameters commonly indicated for description of transport across membranes, since they represent the volume-flow/pressure-gradient ratio ($L_p = J_v/\Delta P$) and the solute-flow/concentration-gradient ratio ($P_s = J_s/\Delta C$). However, L_p and P_s are not intensive or membrane material characteristic parameters since they depend on the membrane geometry (pore radius/porosity and thickness) and structure. Particularly, diffusivity or salt diffusion coefficient (D_s) can be estimated from P_s values if membrane thickness and porosity/partition coefficient are known (for porous/dense membranes) [1]. Moreover, when transport of electrolyte solutions and/or charged particles are involved, membrane fixed charge concentration (X_f) and ion transport numbers ($t_i = I_i/I_T$) as well as other electrochemical characteristic parameters such as ionic diffusion coefficient (D_i), mobility (u_i) and membrane conductivity (λ_m) are also of interest since they give information on the membrane-solution electrical interactions [2]. Membrane thickness is a basic factor for determination of these latter parameters, but it can not be obtained from direct measurements for supported membranes as is usually the structure of ultrafiltration membranes. It is commonly assumed that the support does not affect membrane performance, which may be a valid hypothesis for filtration processes [3], but its contribution in the case of diffusive and electrochemical characterization should not be undoubtedly neglected due to, among other reasons, the unstirred solution layer filling the support, which might cause a certain concentration profile (stagnant layer) and to have a

*Corresponding author.

Presented at the VII Ibero-American Conference on Membrane Science and Technology (CITEM 2010), April 11–14, 2010, Sintra, Portugal

contribution (higher or lower depending on the membrane structure) in the total electrical resistance and concentration gradient. This contribution may be of interest when new membrane applications such as biosensors, contactors or hydrogels for protein encapsulation are considered [4,5], since in those cases the fluxes are associated to electrochemical potential gradients (rather than pressure gradient).

In this paper, the structural and electrochemical characterization of a commercial regenerated cellulose ultrafiltration membrane with a reinforcement support of polypropylene is carried out. Salt diffusion, membrane potential and impedance spectroscopy measurements carried out with the membrane in contact with different NaCl solutions allow the determination of diffusive permeability, ion transport number and electrical resistance. The influence of membrane asymmetry on membrane transport parameters (salt diffusion coefficient and ion transport numbers) was considered by measurements performed for both opposite concentration gradients.

2. Experimental

2.1. Membrane

An ultrafiltration regenerated cellulose membrane with polypropylene reinforcement (RC70PP) with a cut off of 10 kDa from DSS (Naskov, Denmark) was characterized. Membrane thickness was measured with a digital micrometer in six different points covering an area of 30 cm^2 and the value 220 ± 8 μm was obtained, which also includes the polypropylene support. Results obtained with a symmetric regenerated cellulose dialysis membrane with a cut off of 12 kDa and thickness of 120 μm from Medicell International Ltd (England) are also presented for comparison reason (RC-Sy sample).

2.2. Scanning electron microscopy

SEM micrographs of the membrane surfaces were carried out with a Jeol JSM-6400 Scanning Microscopy, working with a voltage of 15 kV. The samples were brought to a gold sputtering process in order to make them conductive.

2.3. X-ray photoelectron spectroscopy analysis

Chemical characterization of the membrane surfaces was carried out by X-ray photoelectron spectroscopy or XPS analysis. XPS spectra were recorded with a Physical Electronics PHI 5700 spectrometer with a multi-channel hemispherical electroanalyzer. MgK_{α}. X-ray was used as excitation sources ($h\nu$ = 1253.6 eV). Accurate ±0.1 eV binding energies were determined with respect to the position of the adventitious C 1s peak at 284.8 eV. High-resolution spectra were recorded at 45° take-off angle by a concentric hemispherical analyzer operating in the constant pass energy mode at 29.35 eV, using a 720 μm diameter analysis area. The residual pressure in the analysis chamber was maintained below 10^{-9} Torr during data acquisition. A PHI ACCESS ESCA-V6.0F software package was used for acquisition and data analysis. Detailed specifications on measurements and analysis procedures are indicated in [6].

2.4. Salt diffusion, membrane potential and impedance spectroscopy measurements

The dead-end test cell used for electrochemical characterization of membranes is similar to that described elsewhere [7]. The membrane was clamped between two glass half-cells by using silicone rubber rings and two magnetic stirrers were placed at the bottom of the half-cells to minimise concentration-polarisation at the membrane surfaces, and measurements were performed at a stirring rate of 525 rpm. Measurements were carried out with the membrane in contact with NaCl solutions at different concentrations, at room temperature (T = (298 ± 1) K) and pH = (5.8 ± 0.3). Before use, the membrane was immersed for around 12 h in the appropriated solution.

The electromotive force (ΔE) between both membrane sides caused by a concentration gradient was measured by connecting two reversible Ag/AgCl electrodes to a digital voltmeter (Yokohama 7552, 1 GΩ input resistance). Measurements were carried out by keeping the concentration of the solution at one side of the membrane constant, c_c = 0.01 M NaCl, and gradually increasing the concentration of the solution at the other side, c_v, from 0.001 M to 0.1 M. These measurements were also carried out in both opposite external conditions: c_c in contact with the regenerated cellulose layer (c_c/RC) or with the polypropylene support (c_c/PP). Membrane potentials were obtained from measured ΔE values by subtraction of the corresponding electrode potential: $\Delta\Phi_{mbr} = \Delta E - (RT/F)\ln(c_v/c_c)$.

Diffusional permeability was determined from salt diffusion measurements which were performed with the membrane separating initially a feed or concentrated solution (c_f) from a diluted or receiving solution (initially distilled water, c_r = 0), and changes in the conductivity of both solutions (λ_f and λ_r) were recorded versus time by means of two conductivity cells (one in each half-cell) connected to two digital conductivity meters (Crison GLP 31). These measurements were performed at different feed concentrations ($0.01 \le c\ (M) \le 0.2$) for both opposite directions: feed concentration in contact with the regenerated cellulose (solution/RC) and the polypropylene support (solution/PP).

Impedance Spectroscopy (IS) measurements were carried using an Impedance Analyzer (Solartron 1260) controlled by a computer in contact with the solution in each half-cell via Ag/AgCl electrodes, and 100 different frequencies in the range 1 Hz10^7 Hz, with a maximum voltage of 0.01 V were recorded. IS data were corrected by software as well as the influence of connecting cables and other parasite capacitances, and the studied system was: electrode // NaCl solution (*c*) // membrane // NaCl solution (*c*) // electrode, having both solutions the same concentration.

2.5. Electrokinetic characterisation of the membrane/solution interface

Streaming potential (SP) gives information on solid/liquid (pore/solution) electrical interface, SP measurements through the membrane were performed with an EKA analyser (Anton Parr, GmBH, Austria), which basically consists of: *i*) two Ag/AgCl electrodes with small holes to permit the solution flows through them and the membrane, and to measure the induced streaming potential; *ii*) a cylindrical cell of 1 cm^2 area; *iii*) a mechanical drive unit to produce and measure the pressure that drives the electrolyte solution from a reservoir into the measuring cell ($7.5 \leq \Delta P$ (kPa) ≤ 30). A more detailed description of the equipment and experimental procedure was presented elsewhere [8]. Measurements were carried out varying the concentration of the solution between 5×10^{-4} M and 7×10^{-3} M at constant pH = (5.8 ± 0.3), and the SP coefficient, $(\Phi_{st} = \Delta V/\Delta P)_{I=0}$, was determined from the average of 10 measurements.

3. Results and discussion

3.1. Scanning electron microscopy and X-ray photoelectron spectroscopy results

Fig. 1 shows SEM micrographs for both surfaces of the RC70PP membrane where the dense RC-layer and the opener structure of the polypropylene (PP) support can clearly be observed. To see the possible effect of that asymmetry on charge and mass transport, measurements for fluxes in both opposite directions were performed.

Chemical characterization of both membranes surfaces membranes was carried out by XPS. The obtained atomic concentrations percentages of the typical elements of both membrane surface materials (carbon and oxygen, since hydrogen is not detected by XPS) are indicated in Table 1, but small percentages of other non-typical elements such nitrogen, silica and chlorine, attributed to contamination (environmental and manufacture), were also found [6,9].

Fig. 2 shows the C1s core level spectra for both membrane surfaces where a narrow and well defined peak at

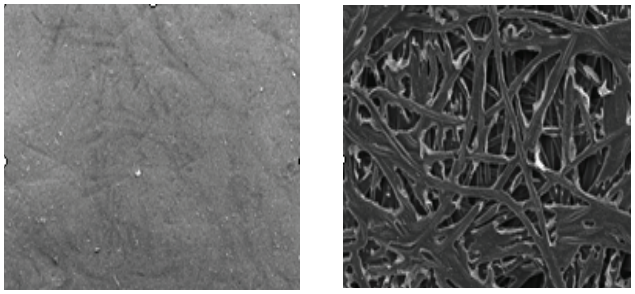

Fig. 1. SEM micrographs of the RC70PP membrane: (a) regenerated cellulose (RC) surface, (b) polypropylene (PP) surface.

Table 1
Atomic concentration percentages of the elements found on both surfaces of the RC70PP membrane by XPS analysis

Sample	C1s (%)	O1s (%)	N1s (%)	Si1s (%)
RC surface	78.4	20.3	0.7	0.5
PP surface	96.5	2.5	0.5	0.2

a bending energy of 285.0 eV (–C–H and –C–C–) for the polypropylene support can be observed, while three different contributions appear when the cellulose layer is analyzed: one peak at 285.0 eV (C_A) and two shoulders, around 286.8 eV (–C–OH and –C–O–C, or C_B) and 288.5 eV (OCO, or C_C), respectively [10,11]. The values obtained for the ratio of oxidized/non-oxidized carbon, $(C_B + C_C)/C_A = 2.4$ and the O/C = 0.26, differ from those corresponding to pure cellulose (5 and 0.83, respectively [12]), due to the oxidation effect of the regeneration process. On the other hand, XPS results seem to indicate that the thicker and interconnected support structure of the polypropylene fibres does not allow the detection of the RC layer.

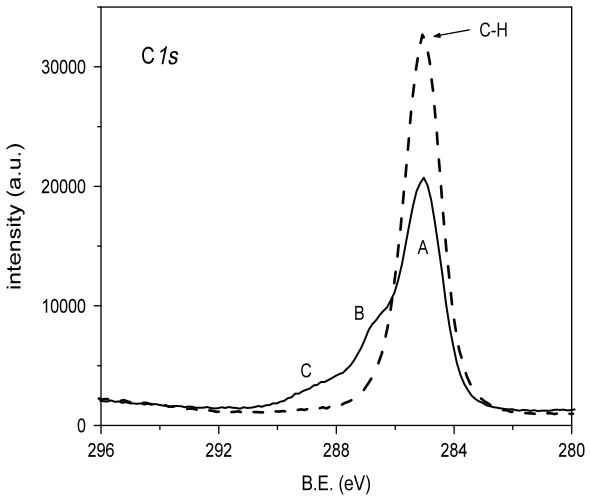

Fig. 2. C1s core level spectra for the membrane RC70PP (Solid line: RC surface; dotted line: PP surface.)

3.2. Electrical characterization results

The transport of ions across the RC70PP membrane was studied by measuring membrane potentials ($\Delta\varphi_{meb}$) for constant concentration 0.01 M NaCl in contact with both RC-layer and PP-support and the obtained values are shown in Fig. 3. As can be observed, some differences were found for opposite external conditions at low concentrations, but similar values were obtained in both cases at high concentrations ($c_v > 0.01$ M). According to the TMS theory, membrane potential can be related with the fixed charge concentration (X_f) and ion transport numbers (t_i) in the membrane by the following expression [13,14]:

$$\Delta\Phi_{mbr} = \frac{w\,RT}{F}\left[U \ln \frac{\sqrt{4y_1^2+1}+wU}{\sqrt{4y_2^2+1}+wU} - \ln \frac{a_2}{a_1}\frac{\sqrt{4y_1^2+1}+w}{\sqrt{4y_2^2+1}+w}\right] \quad (1)$$

where $w = -1$ for negatively charged membranes, $U = t_+ - t_-$ (for 1:1 electrolyte) and $y_i = (a_i\, k/X_f)$, being a_i the solution activity and k the *partition coefficient*; R and F represents the gas and Faraday constant and T is the temperature of the system. A non-linear fit of the experimental values by different iterations allows the determination of X_f, t_+ and γ, and the results are indicated in Table 2. The transport number t_i represents the amount of current transported for one ion (I_i) with respect to the total current crossing the membrane (I_T), that is: $t_i = I_i/I_T$,

Table 2
Fixed charge concentration, X_f, ion transport number, t_+, and partition coefficient, k, determined by Eq. (1) for both opposite experimental situations: constant concentration c_c in contact with the RC-surface or with the PP-support

Flux	X_f (M)	t_+	k
c_c/RC-surface	0.0012	0.379 ± 0.015	1.0
c_c/PP-support	0.0008	0.368 ± 0.012	1.0

for single salts: $t_+ + t_- = 1$; transport number ration, t_+/t_-, is also indicated in Table 2.

Taking into account X_f and t_+ values indicated in Table 2, the RC70PP membrane seems to present a very low electropositive character, oppositely to that usually reported for RC membranes [15–17], and it might be caused by the PP support which could mask the RC layer transport results. The low X_f values obtained support the slight differences obtained at low concentrations, since the free solution charges may screen the effect of membrane charge at high concentrations.

To clarify this point an electrical characterization of membrane/electrolyte interface by SP measurements was carried out. The SP (Δøst) is the electrical potential difference at the two ends of a pore or channel associated to the movement of an electrolyte solution as a result of the application of an external pressure (ΔP), when the steady state is reached, that is for I = 0 [18]. Variation of zeta potential coefficient, $\phi_{st} = (\Delta ø_{st}/\Delta P)_{I=0}$, with electrolyte concentration is shown in Fig. 4, where the electronegative character of the RC70PP membrane can be observed (or more properly, the RC sheet) in agreement with that reported in the literature [19,20], since no electrokinetic effect in the PP support is considered due to

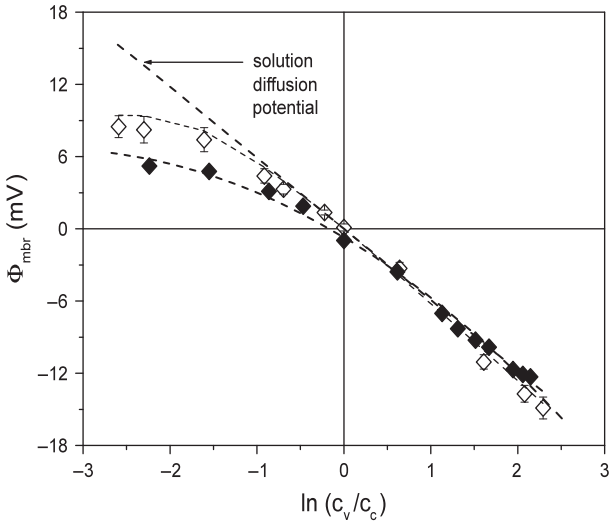

Fig. 3. Membrane potentials versus solution concentrations ratio: (♦) c_c in contact with the RC-layer, (◊) c_c in contact with the polypropylene support (Dashed straight line: solution diffusion potential).

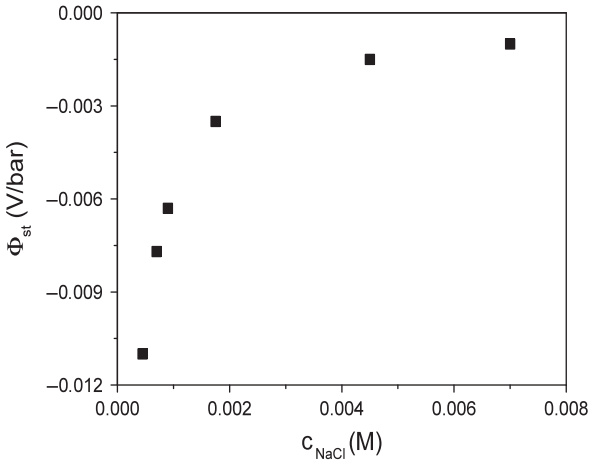

Fig. 4. Streaming potential coefficient, $\Phi_{st} = (\Delta V/\Delta P)_{I=0}$, versus solution concentration.

its open structure [18]. This result seems to confirm the influence of support layers in electrochemical characterization and evidence the need of a detailed description of non-symmetric membranes to get more complete information of their behaviour.

3.3. Diffusion and conductivity results

The flux of solute across a membrane (J_s) at steady-state is related to the concentration gradient at both membrane surfaces (Δc) by the diffusional permeability (P_s):

$$J_s = dn/dt = P_s (c_f - c_r) = P_s \Delta c \quad (2)$$

where P_s values at the different feed solutions studied were determined from the slopes of the conductivity-time relationships taking into account the mass conservation: $c_f^o + c_r^o = c_f^t + c_r^t = cte$, where c_f^o and c_r^o indicate the initial feed and receiving concentrations (at $t = 0$) respectively, while c_f^t and c_r^t represent both concentrations at time t [21]. Fig. 5a shows the diffusional permeability as a function of feed concentration measured for both opposite salt directions, where slight differences depending on the solute flux direction can be observed, which causes a reduction of 5% in the diffusional permeability and it could be related to the stagnant layer and, consequently, a small concentration gradient in the PP-support.

Fig. 5b shows a comparison of concentration dependence for salt diffusion coefficient ($P_s = D_s/\Delta x_m$) obtained for the RC70PP membrane in normal working condition (feed solution in contact with the RC layer), which was calculated assuming three different thickness values: a) Δx_m = 220 μm (total membrane thickness); b) Δx_m = 150 μm (70 % of total membrane thickness); c) Δx_m = 110 μm (50% membrane thickness). For comparison, the values obtained with the commercial RC-Sy symmetric membrane with a known thickness of 120 μm are also shown in Fig. 5b. Since slightly lower diffusion coefficient for the RC70PP membrane than for the RC-Sy one was expected according to the cut off of both samples (10 kDa for the RC70PP and 12 kDa for the RC-Sy), values obtained with the total thickness do not seem to be realistic ($D_s^{RC70PP} > D_s^{RC\text{-}Sy}$), while those determined considering that only half of the RC70PP membrane thickness corresponds to the regenerated cellulose layer (and the other half to the paper support) are significantly low values; however, a thickness of 150 μm (70% of total RC70PP membrane thickness) seems to represent adequately the behaviour of the RC70PP supported membrane.

Membrane electrical resistance was determined from electrochemical impedance spectroscopy (EIS) measurements for the membrane/NaCl solution system and using a model equivalent circuit [22,23]. Impedance

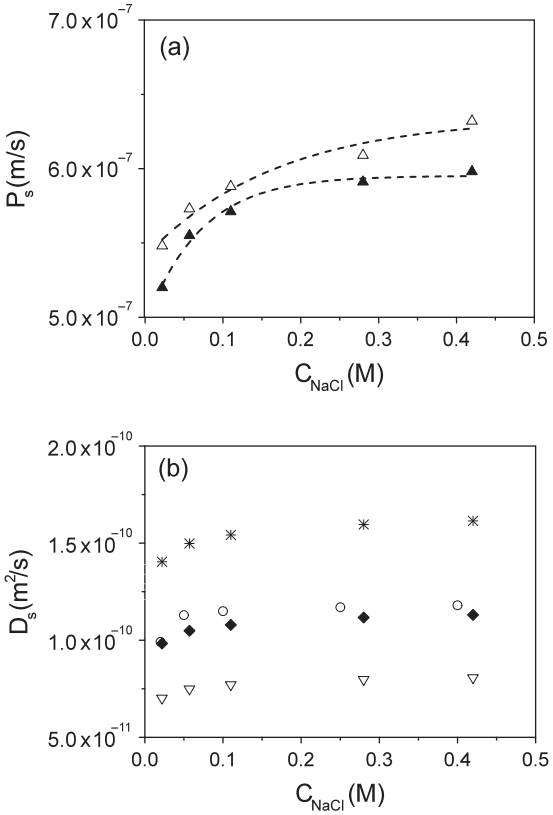

Fig. 5. (a) Diffusional permeability vs NaCl concentration: (▲) solution/RC-layer, (D) solution/PP-support. (b) Salt diffusion coefficient vs NaCl concentration: (*) RC70PP membrane and total thickness, (∇) RC70PP membrane and half thickness, (♦) RC70PP membrane and 70% of total thickness, (o) RC-symmetric membrane (120 μm thickness).

spectroscopy values for the RC70PP membrane in contact with a 0.002 M NaCl solution are shown in Fig. 6a (Nyquist plot, Z_{real} vs $-Z_{img}$) and Fig. 6b (Bode plot, Z_{img} vs frequency); for comparison, impedance plots for the electrolyte solution alone (without membrane) are also indicated in Fig. 6. In both cases a unique relaxation process was obtained (one semi-circle in the diagram shown in Fig. 6a) and the equivalent circuit corresponds to a parallel association of a resistance and a capacitor; ($R_{em}C_{em}$) includes both the membrane itself and the electrolyte solution placed between the membrane and the electrodes, while (R_eC_e) only represents the electrolyte contribution [22,23]. Differences between both membrane-solution and solution systems can also be observed in Fig. 6b, where a shift of the maximum frequency to lower frequency (higher relaxation time) was obtained for the membrane system, which is associated to its more compact structure. The fit of the experimental points by using a non-linear program allows the determination of R_{em} and R_e for each NaCl concentration

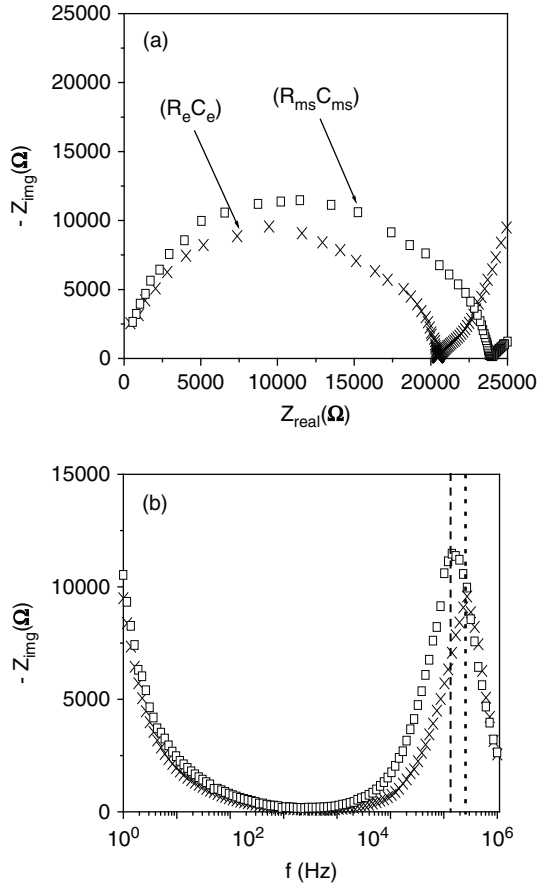

Fig. 6. (a) Nyquist and (b) Bode plots for (□) electrolyte/RC70PP-membrane/electrolyte system and (*x*) electrolyte solution alone (c = 0.002 M).

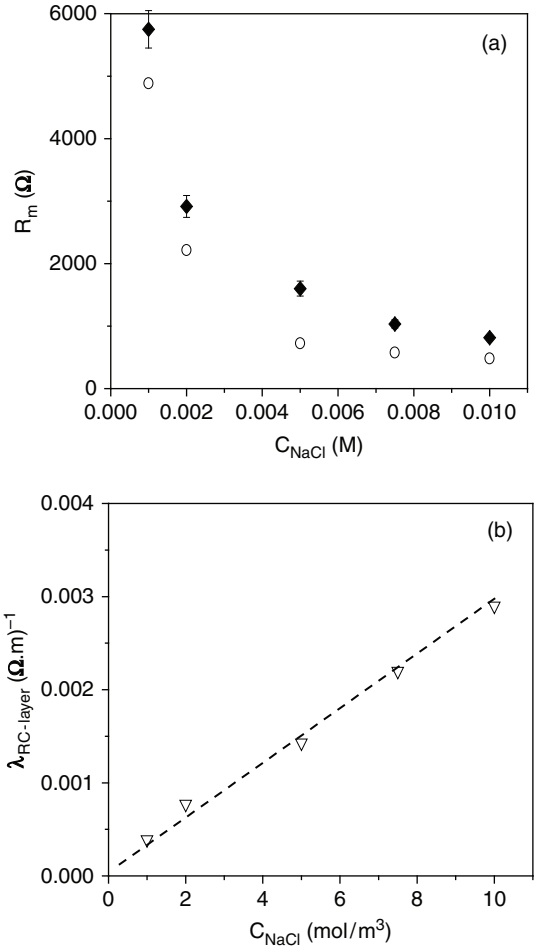

Fig. 7. (a) Membrane electrical resistance as a function of solution concentration: (♦) RC70PP membrane; (o) symmetric RC dialysis membrane (RC-Sy sample). (b) RC-layer conductivity versus solution concentration.

and membrane resistance was obtained by subtraction of these two values: $R_m = R_{em} - R_e$.

Fig. 7a shows the decrease in the R_m values with the increase of NaCl concentration, which is related to the concentration dependence of the electrolyte embedded in the membrane structure; for comparison, values obtained with the symmetrical RC membrane (without any support) are also shown in Fig. 7a, and the same kind of dependence can be observed. The small differences found for both membranes are mainly attributed to the slightly lower cut off and higher thickness of the RC70PP membrane.

Assuming a thickness of 150 μm for the RC-layer, conductivity (λ) values were determined by: $\lambda_{RC\text{-}layer} = \Delta x_{RC}/S \cdot R_{RC}$, where R_{RC} values were obtained from R_m by subtracting the electrical resistance associated to the solution embedded in the PP-layer (around 4% of the total resistance), and its variation with salt concentration is shown in Fig. 7b. Since $\lambda = (F^2/RT) \cdot (D_+ + D) \cdot c$, the slope of the straight line shown in Fig. 7b allows the calculation of $(D_+ + D_-) = 10^{-10}$ m²/s, which is of the same order that the value for D_s obtained from a diffusion measurements (a different set of measurements) and one order of magnitude lower that in solution due to the membrane-solute interactions.

4. Conclusions

Salt diffusion and membrane potential measurements involve concentration gradients and, consequently, exact values of the membrane thickness and solution concentrations at the membrane surfaces are needed for parameters evaluation. However, the unstirred solution embedded in the support layer of ultrafiltration membranes might make difficult such determination, which should affect the correct

calculation of basic electrochemical parameters (salt and ionic diffusion coefficients or ion transport numbers); moreover, the presence of the embedded solution also increases the membrane electrical resistance. This work evidence those effects by comparing electrochemical and electrical results obtained with two regenerated cellulose (RC) membranes with similar cut off, a RC/polypropylene-supported and a RC-symmetric. The set of selected measurements allows a wide characterization of non-symmetric membranes and composite structures for new electrochemical applications.

Acknowledgements

We thank to Junta de Andalucía (project P06-FQM1764), CICYT (project MAT2007-65065, Spain) and European Commission (Project MEMBAQ, 2006–2010) for financial support.

Symbols

a_i	—	solution activity
c_i	—	solution concentration
C_e	—	electrolyte capacitance
C_{em}	—	capacitance for the membrane-electrolyte system
D_s	—	salt difusión coefficient
D_i	—	ionic difusión coefficient
E	—	cell potential
F	—	Faraday constant
I	—	current intensity
J_s	—	solute flow
k	—	partition coefficient
P	—	pressure
P_s	—	diffusion permeability
R	—	gas constant
R_e	—	electrolyte electrical resistance
R_{em}	—	electrical resistance of the membrane-electrolyte system
R_m	—	membrane electrical resistance
S	—	membrane cross section
T	—	temperature
t	—	time
t_i	—	ion transport number or fraction of the total current transport by ion i
V	—	voltage
w	—	sign of the membrane charge
X_f	—	concentration of fixed charge in the membrane
Z_{real}	—	real part of the impedance
Z_{img}	—	imaginary part of the impedance

Greek

Δ	—	difference
Δx_m	—	membrane thickness
Φ_{mbr}	—	membrane potential
Φ_{st}	—	streaming potential coefficient
ϕ_{st}	—	streaming potential
ϕ	—	XPS take off angle
λ_i	—	solution conductivity
$\lambda_{RC\text{-}layer}$	—	conductivity of the regenerated cellulose layer of the RC70PP membrane

References

[1] M. Mulder, Basic Principles of Membrane Technology, Kluwer Academic Publishers, Dordrecht, 1992.
[2] N. Lakshminarayanaiah, Transport Phenomena in Membranes, Academic Press, New York, 1969.
[3] M. Cheryan, Ultrafiltration Handbook, Technomic Publishing Co., Lancaster, 1986.
[4] C.H. Nielsen, Biomimetic membranes for sensor and separation applications, Anal Bioanal Chem., 395 (2009) 697–718.
[5] J. Vogel, M. Perry, J.S. Hansen, P.-Y. Bollinger, C.H. Nielsen and O. Geschke, Support structure for biomimetic applications, J. Micromech. Microeng., 19 (2009) 25–26.
[6] M.J. Ariza, J. Benavente and E. Rodríguez-Castellón, The capability of X-ray photoelectron spectroscopy in the characterization of membranes: Correlation between surface chemical and transport properties in polymeric membranes, (J.M. Wagner, Ed.) Nova Science Publishers, New York, 2009.
[7] C. Torras, X. Zhang, R. García-Valls and J. Benavente, Morphological, Chemical Surface and Electrical Characterizations of Lignosulfonate Modified Membranes, J. Membr. Sci., 297 (2007) 130–137.
[8] A. Cañas, M.J. Ariza and Benavente, J., Characterization of active and porous sublayers of a composite reverse osmosis membrane by impedance spectroscopy, streaming and membrane potentials, salt difusión and X-ray photoelectron spectroscopy measurements, J. Membr. Sci., 183 (2001) 135–142.
[9] J.T.F. Keurentjes, J.G. Harbrecht, D. Brinkman, J.H. Hanemaaijer, M.A. Cohen Stuart and H. van´t Riet, Hydrophobicity measurements of microfiltration and ultrafiltration membranes, J. Membr. Sci., 47 (1989) 333–344.
[10] R.M. France and R.D. Short, Plasma treatment of polymers: the effect of energy transfer from an argon plasma on the surface chemistry of polystyrene and polypropylene. A high-energy resolution X-ray photoelectron spectroscopy study, Langmuir, 14 (1998) 4827–4835.
[11] E. Kontturi, P.C. Thüne and J.W. Niemantsverdriet, Novel method for preparing cellulose model surfaces by spin coating, Polymer 44 (2003) 3621–3627.
[12] U. Freudenberg, S. Zschoche, F. Simon, A. Janke, K. Schmidt, S.H. Behrens, H. Auweter and C. Werner, Covalent immobilization of cellulose layers onto maleic anhydride copolymer thin films, Biomacromolecules, 6 (2005) 1628–1636.
[13] T. Teorell, Transport phenomena in membranes, Discuss. Faraday Soc., 21 (1956) 9.
[14] K.H. Meyer and J.F. Sievers, La permeabilité des membranes. I. Theorie de la permabilité ionique, Helv. Chim. Acta, 19 (1936) 646.
[15] C.J. van Oss, Ultrafiltration membrane performance, Science, 139 (1963) 1123–1124
[16] Y. Kimura, H.-J. Lim and T. Ijima, Membrane potential of charged cellulosic membranes, J. Membr. Sci., 18 (1984) 285–293.
[17] J.D. Ramos, C. Milano, V. Romero, S. Escalera, M.C. Alba, M.I. Vázquez and J. Benavente, Water effect on physical-chemical and elastic parameters for a dense cellulose regenerated

membranes. Transport of different aqueous electrolyte solutions, J. Membr. Sci., 352 (2010) 153–159.
[18] R.J. Hunter, Zeta Potencial in Colloid Science. Principles and Applications, Academia Press, London, 1998.
[19] M. Pointié, Effect of aging on UF membranes by a streaming potential (SP) method, J. Membr. Sci., 154 (1999) 213–220.
[20] A. Cañas, M.J. Ariza and J. Benavente, A comparison of electrochemical and electrokinetic parameters determined for cellophane membranes in contact with NaCl and $NaNO_3$ solutions, J. Colloid Interface Sic., 246 (2002) 150–156.
[21] D. Gilbert, T. Okano, T. Miyata and S.W. Kim, Macromolecular diffusion through collagen membranes, Int. J. Pharm., 47 (1988) 79.
[22] A. Asaka, Dielectric properties of cellulose acetate reverse osmosis membranes in aqueous salt solutions, J. Membr. Sci., 50 (1990) 7180.
[23] J. Benavente, Electrical characterization of membranes, in Monitoring and Visualizing Membrane-Based Process (C. Güell, M. Ferrando, and F. López, Eds.), Wiley-VCH, 2009.